Technical Report
RAL-TR-2000-051

CLRC

A New Model for Electron Ranges in Solid Materials

J E Bateman

6th December 2000

COUNCIL FOR THE CENTRAL LABORATORY OF THE RESEARCH COUNCILS

The Central Laboratory of the Research Councils
Library and Information Services
Rutherford Appleton Laboratory
Chilton
Didcot
Oxfordshire
OX11 0QX
Tel: 01235 445384 Fax: 01235 446403
E-mail library@rl.ac.uk

ISSN 1358-6254

RAL-TR-2000-051

A NEW MODEL FOR ELECTRON RANGES IN SOLID MATERIALS

J.E. Bateman

Rutherford Appleton Laboratory, Chilton, Didcot, Oxon, OX11 0QX, UK

22 November 2000

Abstract

A new definition is proposed for the range of fast (1keV – 50keV) electrons in solid materials: the *spherical range*. Associated with a simple model it permits calculation of the transmission of electrons through foils and the escape efficiency of electron yield measurements in surface studies such as x-ray absorption fine structure. For materials of moderate to high atomic number (Z>25) the spherical range takes better account of the effects of elastic scattering on the range than the usual *extrapolated range* parameter.

1. Introduction

The range (R_0) of a heavy charged particle, such as a proton, is a well-defined quantity which is seen experimentally as the mode of the histogram of the stopping distances of the particles in a pencil beam of energy E_0 incident on a given material. The histogram has an approximately normal distribution about R_0 showing that the process is dominated by a large number of small inelastic scattering events. Small tails to the normal distribution are caused by second order processes such as nuclear scattering, which produces tailing to low ranges and charge pickup at the end of the range, which causes tailing to higher ranges.

The Bethe-Block model for the small inelastic scattering [1] is used to evaluate the specific energy loss S(E) = dE/dx of a charged particle as a function of it's energy (or velocity) and the range R_0 can be evaluated using the relation:

$$R_0(E_0) = \int_{E_T}^{E_0} \frac{dE}{S(E)} \qquad (1)$$

where E_T is an appropriate lower energy threshold (≈10eV). The standard deviation of the normal distribution (known as the range straggling) is typically ≈1% of the range. For example protons of 2 Mev exhibit range straggling of 1.97% in aluminium [2].

A standard experimental method for measuring the range of charged particles involves measuring the fraction of a pencil beam transmitted through a series of foils, T(R). This is mathematically equivalent to:

$$T(R) = 1 - \frac{1}{N_0}\int_0^R \frac{dN}{dR} dR \qquad (2)$$

where N_0 is the number of electrons in the incident beam and dN/dR is the distribution of particle ranges. Equation (2) results in a quasi-step function (actually the complementary error function) with the value of the foil thickness at T=50% giving R_0.

As figure 1 shows [3,4,5], measuring the range of electrons using this technique results in very different curves from the simple step functions observed with protons. Depending on the energy and the material, the transmission curves can vary from concave-up to concave-down with no sign of a step which may be used to define R_0. In practice, a *practical* or *extrapolated range* (R_x) is defined by finding a straight-line portion of the transmission curve and extrapolating it to cut the range axis. This intercept value is taken to be R_x. However, as figure 1 demonstrates, this is a fairly arbitrary and error-prone procedure in many cases since, in the absence of an inflexion in the curve there is often no obvious portion of the curve whose gradient may be used.

As pointed out by Coslett and Thomas [4], this behaviour is caused by the intense elastic scattering experienced by electrons in solid materials as a result of their very high charge to mass ratio. The result of this effect is that the *extrapolated range* R_x is

found, in many materials, to be as little as 50% of the *maximum range* R_0 as defined by equation (1). This paper proposes a new definition for the electron range which takes account of the elastic scattering process and yields a consistent parameter which is useful for practical application in the calculation of electron yields from converter foils for x-rays and the escape yield of auger and photoelectrons from the surface of solid samples. This model assumes that the elastic scattering is sufficiently intense that the initial direction of the electron is completely lost within a short fraction of its maximum range and that the end points of the electron paths are distributed over a sphere of radius R_s where R_s is defined as the spherical range. The transmission curve is now determined simply by the intersection of this sphere with the external surface of the material.

2. **The Model**

The model for the *spherical range* (R_s) of an electron was evolved in the course of an extensive program of work covering the development of hybrid x-ray and gamma ray detectors in which the incident radiation was converted into fast electrons in the walls of a channel plate electron multiplier [6] or in metal foils placed within the gas volume of a multiwire proportional counter [7,8]. Since high Z materials were being used (Sn, Pb) it was assumed that the weak directionality of the photoelectrons produced would be lost due to the elastic scattering processes and that the electron range endpoints would be isotropically distributed enabling a simple geometric determination of the fraction escaping the surface.

In figure 2 a source of monoenergetic electrons is located at a depth x below the surface of the solid material. According to the simplest form of the model, the end-points of the electron paths are uniformly distributed on the surface of a sphere of radius R_s. (Strictly, one is interested in the maximum distances the electron reaches from the source point. This will often be greater than the distance of the final end-point of the track from the source; however, it is convenient to use the term end-point.) From simple geometry, the fraction escaping the surface is just the solid angle contained in the cone with polar angle θ_{max}, i.e. $(1 - \cos\theta_{max})/2$ where $\cos\theta_{max}=x/R_s$. For the case of x-rays converting in thin foils of thickness W, this escape fraction can be averaged over the thickness of the foil to give the escape yield of the conversion electrons (ε): $\varepsilon=R_s/2W$ for $R_s \leq W$ and $\varepsilon=1-W/2Rs$ for $R_s>W$. Using the R_x values collated by Tabata, Ito and Okabe [9] for R_s, it was found that a reasonable level of agreement existed between the model and experimental measurements. The model was used extensively in design studies for hybrid gas detectors for x-rays and gamma rays[7,8].

The suitability of the model for electrons generated within a material is obvious. Less clear is its possible application to (or comparison with) electron range measurements performed with pencil beams in which the source of electrons is highly directional. If one assumes that a directional beam of electrons incident on a foil of thickness x is thoroughly randomised by the elastic scattering process within the thickness of the foil then the transmission of the foil just becomes:

$$T(x) = 1 - \frac{x}{R_s} \qquad (3)$$

and a transmission curve linear in x is predicted. Comparison with the transmission curves measured by Schonland [5] for aluminium (figure 3) shows that for Al in this electron energy range (14keV – 41keV) surprisingly linear curves are in fact demonstrated. The ease of finding a straight line to extrapolate means that in this case one finds little difference between the values of R_s and R_x.

The unfitted high range tails seen in the transmission curves in figure 3 point the way to the first necessary elaboration of the simple model. So far the radial distribution of electron track end-points has been assumed to be a delta function. This is clearly simplistic. The scattering processes will inevitably produce a spread, which, due to the large numbers of scatters (≈100) may be expected to be a normal distribution. This modification to equation (3) does not lead to a simple analytical solution; however it is simple to model the escape of the electrons using a Monte Carlo computer program. In the program rays are generated isotropically in the hemisphere towards the surface and events are added to the transmitted sample if $R_s^* \cos\theta > x$ (see figure 2). Here x is the foil thickness and R_s^* is a normally distributed spherical range value. This process introduces a new parameter, the standard deviation (SD) of the range distribution into the fitting process. It is found appropriate to use the relative SD (the SD expressed as a function of the mode) and this is identified as σ_{rel}.

In the fitting process R_s and σ_{rel} are adjusted until the best fit is obtained to the experimental data. Figure 4 shows the results of this process as applied to the aluminium transmission curves of figure 3. The ripples on the fit curves are simply due to the statistical noise of the Monte Carlo process. As expected the ratio of R_x to R_s is very close to unity. σ_{rel} is almost constant over the electron energy range at 15%.

Figure 5 shows the copper transmission data of Coslett and Thomas [4] over an electron energy range of 4keV to 16keV. The ability of the spherical range model to fit transmission curves with no straight-line sections is demonstrated. In this case it is noticeable that σ_{rel} is much bigger than for aluminium (30%) and increases as the electron energy decreases. As discussed below, this is understandable in view of the energy and Z (atomic number of the material) dependence of the electron elastic scattering cross-section ($\sigma_e \propto Z^2/E$ [4]). A systematic energy dependence is also noticed in the R_x/R_s ratio with R_s dropping to $0.8R_x$ at 4keV.

The gold transmission data in figure 6 [4] shows the same trends continuing as the Z of the material increases. The model shows that σ_{rel} is now 50% over the electron energy range (4keV – 20keV) and the spherical range is now systematically lower than the projected range, dropping to $0.56R_x$ at 4keV.

In low Z materials such as carbon (Z=6), the elastic scattering cross-section is reduced relative to the inelastic one. This means that the directions of the electrons in a pencil beam may not be fully randomised. The spherical model can take account of this by restricting the range of the polar angle (θ) of the rays initially generated. Thus instead of generating isotropic rays over the range $0<\cos\theta<1$ the program generates them over the range $C_{min}<\cos\theta<1$. The transition is smoothed by convolving the $\cos\theta$ values with a normal distribution with standard deviation σ_C.

Figure 7 shows the transmission data obtained by Lane and Zaffarano [3] for electrons between 3.3keV and 8keV in collodion. In this case the model is set to have $\sigma_C = C_{min}$. The model now fits the experimental data quite well. The reduced significance of the elastic scattering is made clear by the small value of σ_{rel} (5%) and the R_x/R_s ratio of near unity (1.05). The minimum cosθ value, C_{min} ($=\sigma_C$) varies systematically with the electron energy taking account of the changing relative magnitude of the elastic and inelastic scattering processes.

In higher Z materials such as aluminium (Z=13) and copper (Z=29) the very lowest energy transmission curves (figures 4,5) show clear signs of a concave down portion near x = 0. This can be interpreted as being due to the fact that the number of elastic scatters possible in the foil is not enough to randomise the electron directions. The version of the model with the cosθ cut-off is capable of fitting these data sets.

At very high electron energies (159keV – 336keV) the inelastic cross-section decreases and the transmission curves of Seliger [10] for aluminium (figure 8) resemble the collodion curves at low energies. The inflexion in the curves is used to define R_x. The version of the spherical range model with the cosθ cut-off fits the experimental data very well. In this case C_{min} varies systematically with the electron energy (as with the collodion data) but in this case σ_C (=0.44) is essentially independent of energy. Figure 8 gives the details. The value of σ_{rel} is 15%, consistent with the lower energy data (figure 4) and the R_x/R_s ratio is less than unity by about 20% varying slowly with electron energy.

An experimentally convenient method for measuring electron ranges in solid materials is to measure the transmission of monoenergetic electrons through a series of foils of thickness W as the beam energy is varied [11]. Figure 9 shows the copper data from Coslett and Thomas displayed in this way. The extrapolated range R_x is derived by finding the steepest gradient on each curve and extrapolating it to the energy axis where the intercept gives the energy corresponding to the range W.

The spherical model prediction for the transmission is easily obtained by rewriting equation (4):

$$T(E) = 1 - \frac{W}{R_s(E)} \qquad (4)$$

Fitting equation (4) has the obvious problem that in order to proceed it is necessary to specify the functional form of the range energy curve. This is clearly unsatisfactory. Figure 9 shows the fits obtained assuming a function of the form $R_s(E) = aE^b$. A further complication evident from the previous analysis is that σ_{rel} is a function of electron energy which must be hypothesised. In figure 9 the Monte Carlo model has σ_{rel}=0.33 throughout. The program performs essentially as before with R_s defined by the incident electron energy according to the function stated above.

The smooth line through the data points for W=0.024μm shows the fit using the simplest form of the model (σ_{rel}=0) and it describes most of the data satisfactorily. At greater foil thicknesses the effect of the dispersion on R_s demands the next level of the

model with σ_{rel}=0.33. While the model clearly reproduces the essential behaviour of the data, universal fits cannot be easily obtained. Data presented in this format should be re-plotted in the form of figure 5 before attempting to fit with the model.

3. Comparison of the *spherical* and *extrapolated* ranges

The spherical range model has been used throughout recent work on modelling the sensitivity and linearity of experiments which analyse X-ray Absorption Fine Structure (XAFS) using the electron yield from a surface [12]. In this modelling the value used for R_s was in fact the extrapolated range R_x as collated by Tabata Ito and Okabe [9], which is, in turn, based on the data sets used in the analyses presented above. Given the rather vague definition of R_x, the question arose as to the validity of this proceeding, since the sensitivity, linearity and probe depth of surface XAFS analysis (using electron yield) are directly dependent on the electron range. This query led to the investigation of the original range data to see if R_s and R_x are comparable and if it is acceptable to use R_x in the spherical model. The fits presented above permit a comparison of the ranges over a reasonable range of atomic number.

Collodion ($Z\approx6$)
Figure 7 shows that the model consistently fits the collodion data with R_x/R_s=1.05. Given a three parameter fit with relatively sparse and noisy data, this is consistent with R_x=R_s. There is no sign of any energy-dependence of the ratio over the range 3.3keV to 8keV.

Aluminium (Z=13)
In the energy range 14keV – 41keV (figure 4) R_x/R_s has a mean value of 0.97 with an RMS error of 0.024 and no sign of a systematic trend with energy.

In the higher energy range of 159keV – 336keV (figure 8) there is sign of a consistent upward trend in the ratio R_x/R_s (0.78 to 0.85).

Copper (Z=29)
Figure 10 shows R_x and R_s plotted for copper in the energy range 4keV – 16keV. The fits of Tabata Ito and Okabe [9] follow tabulated data for Rx from Coslett and Thomas [4]. The R_s data is derived by the Monte Carlo model from the transmission curves, also published by Coslett and Thomas [4]. In this case a systematic and noise-free divergence is noted between R_x and R_s with R_s significantly lower than R_x at the lower energies. The R_s points fit very well to the function $R_s = 0.006596E^{1.6327}$. If this function is extrapolated to electron energies below 1keV the predicted divergence is greater than a factor of two.

Gold (Z=79)
Figure 11 shows R_x and R_s plotted from the Coslett and Thomas data for gold in the energy range 4keV – 20keV [4]. In this case R_s is seen to lie significantly below R_x over the whole range and the power law fit indicates that at energies below 1keV the discrepancy becomes greater than a factor of three.

Although the available data is rather sparse in Z to permit a detailed analysis, figure 12 shows that R_x/R_s has a consistent pattern of behaviour with energy and the atomic

number of the material. The magnitude of the effect seems to rise approximately linearly with Z and increases rapidly as E decreases. These trends are consistent with the behaviour of the elastic scattering cross-section ($\sigma_e \propto Z^2/E$ [4]) and reinforce the belief that at high Z and low E, R_s is a more realistic measure of the electron range than R_x.

With the exception of the low end of the copper electron energy range, the relative SD of R_s (σ_{rel}) shows very little dependence on the electron energy in the ranges available. The reason for the exception in the case of copper is not understood. Figure 13 shows that the variance of R_s (σ_{rel}^2) is proportional to Z^2/A a linear relationship is obtained. Since Z^2/A is proportional to the most probable scattering angle in a model of multiple elastic scattering [4] this graph provides a clear illustration of the role of the elastic scattering in determining the distribution of the electron track endpoints.

4. Application of the *spherical range* to XAFS modelling

In x-ray absorption fine structure studies the detection of the auger electron yield is a favoured method for the characterisation of surface structures such as catalytic layers [13]. This is due to the short range of the auger products of an excited atom compared to that of the fluorescent x-rays. The probe depth of the x-ray beam is thus defined essentially by the range of the auger electrons which is typically 10nm – 100nm in the soft x-ray region. As shown elsewhere [12], the sensitivity and linearity of the measurement process is determined by the dimensionless parameter $u = \mu R/\sin\phi$, where μ is the linear absorption coefficient of the incident x-rays, R is the electron range in the material and ϕ is the glancing angle of incidence of the beam on the sample. For values of $u < 0.1$ the detected electron yield is proportional to μ, the parameter carrying the structural information and the fraction of the generated auger signal is approximately u/4. At values of $u > 0.1$ the electron yield progressively saturates and the structural information is suppressed. This situation can develop (for example) when using the L shell emission from a transition element when the value of μ can approach 1/R for the emitted augers. Thus the values used for the electron range of a particular auger electron directly affects any estimate of the sampling depth, the sensitivity and linearity of the XAFS measurement.

A model of the XAFS process (using the electron yield) has been developed using the concept of the spherical range and using equation (3) to estimate the escape yield of electrons generated in a layer dx at a depth x below the surface. Integration of this factor multiplied by the number of augers generated in this layer gives the electron yield counting rate relative to the incident beam [12]. The analytical XAFS model uses the simplest version of the spherical range model with $\sigma_{rel}=0$. Use of the fitted spherical range data with a finite value of σ_{rel} requires that the integration be carried out via a Monte Carlo program.

Figure 14 shows the predicted escape efficiency (ε_A, the fraction of generated augers which escape from the surface of a semi-infinite slab) as a function of μ in the range of μ sampled just above the K shell edge of nickel. The upper curve (squares) is the simplest model ($\sigma_{rel} = 0$) with R_x used for the auger range; the lower curves represent the predictions with R_s used and $\sigma_{rel} = 0$ (triangles) and R_s with $\sigma_{rel} = 0.4$ (circles).

The values of R_s and σ_{rel} are those fitted for copper above. The lower value of R_s relative to R_x reduces the predicted sensitivity proportionately (in the linear region) and accordingly improves the linearity slightly at a given value of μ. The addition of the spread in R_s ($\sigma_{rel} = 0.4$) is seen to make very little difference to the predicted sensitivity or linearity. A straight line fit to the linear region of one of the curves is included to highlight the non-linearity of the response at the highest μ values.

Some conclusions can be drawn from figures 14 and 12:

- It is possible to achieve accuracy of a few % in the XAFS modelling without taking account of the spread of R_s even when σ_{rel} is large ($\approx$0.5) in the case of high Z materials. This means that the analytical formula derived via equation (3) may be used with confidence.

- For high Z materials at low energies, the significant decrease of R_s relative to R_x displaces the $\varepsilon_A(u)$ curve significantly resulting in lower predicted sensitivity and improved linearity.

- Since R_s determines the sampling depth in the surface of the material, the spherical range model predicts significantly shallower sampling depths in high Z materials at low electron energies.

- Tests in which the Monte Carlo model was run to determine the depth profile of the escaping electrons for the nickel surface with σ_{rel}=0.4 showed that the profile was negligibly different from the $\sigma_{rel} = 0$ case. Thus the simple, analytical version of the model is adequate in this respect also.

In recent experimental tests the electron yield energy spectrum from a nickel surface placed inside a gas microstrip detector was measured [14]. Figure 15 shows the energy spectrum of the escaping augers with the x-ray beam energy just below (lower curve) and just above (upper curve) the K shell edge. A Monte Carlo version of the simplest model was used to generate the residual ranges of the escaping electrons and hence their residual energies. The marked curves show that the model reproduces the corresponding energy spectra quite faithfully. The extra distributions at the low energy end of the experimental spectra are due to L shell fluorescence and secondaries from the surface. The contribution of the L shell photoelectrons is included in the model but the small amount of contamination by the x-ray beam at the upper edge is not.

5. Limitations of the model

In the parameter ranges 2keV < E < 50keV and Z > 13 the spherical range model fits the transmission data available with only two parameters, the spherical range R_s and its relative standard deviation σ_{rel}. When the Z of the material is low, as for collodion, or, for high Z materials, the electron energy is high (>50keV) a further refinement which limits the cone of rays is necessary to describe the transmission data. The boundary between these two domains is clearly set by the number of elastic scattering events in the depth of material used. This must be great enough to ensure the

randomisation of the electron directions which the model assumes. In this domain the systematic behaviour of R_s with respect to R_x (the extrapolated range), encourages the belief that R_s takes better account of the elastic scattering contribution to the range than does R_x. The unimportance of σ_{rel} in the modelling of electron emission from surfaces in XAFS removes the need to take account of a second parameter (σ_{rel}) so that simple analytical forms can be used with confidence.

When the angular distribution of rays is adjusted to take account of the low elastic scattering in the model for the collodion data, the resulting R_s values are very close to the standard R_x values (-5%) and not sensitive to E. This finding agrees with expectations for low Z materials in which the inelastic processes become dominant. The simple geometric model will not describe the transmission of a pencil beam, but in the case of an isotropic (or quasi-isotropic) source of electrons in the material below a surface, the spherical geometry is imposed by the source distribution and the simple model will be useful. The evidence is that R_x can be used as the appropriate range parameter.

At high electron energies in aluminium it was possible to model the transmission data with a proliferation of parameters which take account of the loss of isoptropy caused by the elastic scattering cross-section falling with energy. What significance can be attached to the +20% deviation of the fitted R_s to the standard value of R_x is uncertain. In this energy region the photoelectrons are generated in a material by the photoelectric effect and the compton effect. Near photon energies of 100keV the fast electrons are not highly directional but as the photon energy increases above this value strong peaking in the direction of the incident photon vector occurs. Thus up to photon energies of a few hundred keV it is probably reasonable to assume isotropic electron emission in high Z materials (Z>50) and use the simple model with the standard values of R_x.

Figure 15 shows that the simple spherical range model can reproduce the energy spectrum of the augers emitted from a surface. In this case the original source of the electrons is isotropic. When, on the other hand, the energy spectrum is compared with the measured spectra obtained with a pencil beam [4] large discrepancies are observed. In particular, the peak energy is systematically lower in the simple spherical model. Use of the model to generate energy spectra must therefore be reserved to cases in which the original electron emission is isotropic.

6. Discussion

When a fast electron stops in a material it pursues a random walk dominated by two distinct processes: inelastic scatters which rob it of energy with small deflections and elastic scatters which preserve the energy but which can scatter it through significant angles. The result is a path which for keV electrons can curl up quite tightly and the experimental evidence for this is that measurements of R_x can easily be $<50\%R_0$ (as defined by equation (1). This behaviour is dictated by the elastic (Rutherford) scattering cross-section $\sigma_e \propto Z^2/E$ [4], i.e. maximal effects are expected with low energy electrons stopping in high (or moderately high) Z materials. In applications such x-ray conversion in foils and electron yield XAFS, the generation of the fast electrons within the material is isotropic or quasi-isotropic and the interesting

parameter is the fraction of electrons which escape the surface into a detector of some description. In other words it is only the track end-points in which one is interested. The conditions specified clearly dictate a spherically-symmetric distribution of end-points which (allowing for the stochastic processes) will have a normal radial distribution with a mode R_s and a relative variance σ_{rel}^2.

When the source of the electrons approaches the surface of a material ($x < R_s$ in figure 2) some of the end-points lie outside the surface so that the escaping fraction can be deduced from the solid angle of the cone of polar angle $\cos^{-1}(x/R_s)$. As x approaches the surface the symmetry of the spherical distribution is disturbed and more than 50% of the electrons will appear outside the surface when x=0. A detailed physical simulation of the electron escape process by Schroeder [15] shows that, almost independent of Z and E (3keV – 7.5keV) ≈50% of the electrons emitted backwards into the sample from a source at x=0 are scattered out of the sample. This effect makes the escape fraction vary rather like a negative exponential function as a function of x instead of the linear function described by equation (3). However, on integrating up the distributions over the total sensitive depth (x) the difference between the predicted escape fractions is in the range of a few %.

In applying this model to the estimation of the sensitivity of XAFS measurements on nickel surface layers [14] the question arose as to validity of using the standard parameterisation of the extrapolated range R_x [9] for the new notional spherical range R_s. The measurements of R_x are conventionally performed in planar geometry on foils of specified thickness with pencil beams of electrons making it improbable, at first glance, that the spherical model would have any relevance. However, inspection of the aluminium data shown in figure 3 showed that, with the exception of small tails at long ranges, the transmission data was very suggestive of plausible fits to equation (3). The tails could be fitted with a plausible variance assigned to R_s. The same model successfully fits the experimental transmission data for copper and gold in the energy range 4keV to 20keV (figures 5 and 6).

The success of these fits implies that the initial directions of the electrons have been thoroughly randomised by the hundred or so elastic scattering interactions experienced in even the thinnest foils used, so producing the effect of an isotropic source. The failure of the model to fit the collodion data (figure 7) and the high energy data in aluminium (figure 8) without artificial restriction of the cone of rays ties up with the behaviour of the elastic scattering cross-section, $\sigma_e \propto Z^2/E$. In these cases there are insufficient elastic scattering lengths in the typical range to completely erase the original direction of the electron beam. It is thus concluded that in the range of atomic number in which the elastic scattering dominates the inelastic processes ($Z \geq 13$) and in the energy range of the data (4keV to 20keV) R_s is a valid concept.

The data shows that for atomic numbers up to around that of aluminium there is no significant difference between the tabulated values of R_x and R_s derived from the fits. However, as Z increases to the region of copper strong systematic deviations become evident with R_s consistently lower than R_x. The data is limited to a lower threshold of 4keV; however, fits of the form $R_s = aE^b$ to the copper and gold data (figures 10 and 11) imply that discrepancies of more than a factor of two can arise below electron energies of 1keV. This behaviour is consistent with the increasing influence of the elastic scattering processes as the energy decreases. Thus while at E = 10keV there

will be discrepancies of a few tens of percent between R_x and R_s, at 1keV and below the discrepancy can reach a factor of two or three. As shown above, in the XAFS calculations, this factor feeds directly into the predicted sensitivity and, more importantly into the probe depth of the analysis.

Due to the great difficulty of experimental range measurements with sub-keV electron beams, reliance is generally placed on theoretical calculations of the specific energy loss, based on the measured optical constants of the material. Such a calculation (the continuously slowing down approximation – CSDA) for gold [16] is shown in figure 11. Using equation (1) this approach evaluates R_0, the maximum range with no account taken of the elastic scattering. For low Z materials ($Z \approx 6$) this will be a reasonable approximation. However, in the case of gold at 1keV (as figure 11 shows) R_0 is already a factor of two greater than R_x, and a factor of six greater than R_s. The present work indicates that R_s is the most reliable range parameter for calculating the x-ray electron yields of surfaces. Recent x-ray magnetic circular dichroism (XMCD) measurements in which a form of XAFS was performed on cobalt samples using the electron yield of cobalt L shell augers ($\approx$680eV) [17] showed a reasonably linear electron yield dependence on μ. If either R_x or R_0 are substituted into the XAFS model for the electron yield, serious saturation of the response is predicted, while R_s predicts a small degree of saturation, which is consistent with the experimental observations.

7. Conclusion

In the electron energy range of general interest in XAFS studies (1keV<E<20keV), it has been shown that the spherical range R_s of a fast electron is a useful concept which takes better account of the effects of elastic scattering on the transmission of electrons through foils and surfaces than the commonly defined projected range R_x. In materials of moderate to high atomic number (Z>25) R_s deviates significantly from R_x at low energies (<5keV) and is believed to be a more realistic measure.

The associated model for the escape efficiency of the electron from a solid interface permits good fitting of transmission data for Z>13 and facilitates simple and effective modelling of electron yields from surface XAFS studies.

References

1. See, for example, D. Ritson, Techniques of high energy physics, Interscience, New York 1971.

2. R.M. Sternheimer, Phys. Rev. **117**, 485 (1960)

3. R.O. Lane and D.J. Zaffarano, Phys. Rev. **94**, 960 (1954)

4. V.E. Coslett and R.N. Thomas, Brit. J. Appl. Phys. **15**, 883 (1964)
   V.E. Coslett and R.N. Thomas, Brit. J. Appl. Phys. **15**, 1283 (1964)

5. B.F.J. Schonland, Proc. Royal Soc. Of London **A104**, 235 (1923)

6. J.E. Bateman, Nucl. Instr. & Meth. **144**, 537 (1977)

7. J.E. Bateman and J.F. Connolly, Phys. Med. Biol. **23**, 455 (1978)

8. J.E. Bateman, J.F Connolly, R. Stephenson, G.J. Tappern and A.C. Flesher, Nucl. Instr. & Meth. **225**, 209 (1984)

9. T. Tabata, R. Ito and S. Okabe, Nucl. Instr. & Meth. **103**, 85 (1972)

10. H. H. Seliger, Phys. Rev. **100**, 1029 (1955)

11. H. Kanter and E.J. Sternglass, Phys. Rev. **126** 620 (1962)

12. J.E. Bateman, Surface EXAFS – A mathematical model, Rutherford Appleton Laboratory report, RAL-TR-2000-052 (http://www-dienst.rl.ac.uk/library/2000/tr/raltr-2000052.pdf)

13. X-ray absorption fine structure for catalysts and surfaces, Y. Iwasawa (Ed.), World Scientific, Singapore, 1996

14. T. Rayment, S.L.M. Schroeder, R.M. Lambert, G.D. Moggridge, J.E Bateman, G.E. Derbyshire and R. Stephenson, Auger electron detection at ambient pressures for x-ray absorption spectroscopy. (to be published)

15. S.L.M. Schroeder, Solid State Communications, **98**, 405 (1996)

16. J.C. Ashley, C.J. Tung, R.H. Richie and V.E. Anderson, IEEE Trans. Nucl. Sci. **NS-23**, 1833 (1976)

17. J.E. Bateman, G.E. Derbyshire, E. Dudzik, G. van der Laan, J.D. Lipp, A. D. Smith and R. Stephenson, A new x-ray detector for magnetic circular dichroism experiments, presented at SRI2000, Berlin, August 2000 (to be published in Nucl. Instr. and Meth.) also Rutherford Appleton Laboratory report, http://www-dienst.rl.ac.uk/library/2000/tr/raltr-2000041.pdf

Figure Captions

1. The fraction of electrons of energy E transmitted through foils of thickness W where W is expressed as a fraction of the Bethe-Block range R_0 as defined by equation (1). Typical curves for materials of various atomic numbers (Z) are shown. The data comes from references [3], [4] and [5].

2. Schematic diagram for the definition of the *spherical range* of a fast electron. A source of isotropically radiating monochromatic electrons is envisaged at a depth x below the surface of a material. Electrons are assumed to escape when $\theta < \cos^{-1}(x/R_s)$.

3. The electron transmission data of Schonland [5] for aluminium at four electron energies (E) with the fits of the simplest form of the *spherical range* model applied.

4. The Schonland data of figure 3 with a normal distribution applied to the *spherical range* R_s before evaluation of the fraction of electrons escaping from the surface. The ratio of the standard *extrapolated range* R_x [9] and the *spherical range* Rs and the relative standard deviation of R_s (σ_{rel}) are shown for each electron energy E.

5. The *spherical range* model fits to the transmission data of Coslett and Thomas [4] for a range of electron energies in copper. The values of R_x/R_s and σ_{rel} for each electron energy are shown in the legends.

6. The *spherical range* model fits to the transmission data of Coslett and Thomas [4] for a range of electron energies in gold. The values of R_x/R_s and σ_{rel} for each electron energy are shown in the legends.

7. The modified *spherical range* model fits to the transmission data of Lane and Zaffarano [3] for a range of electron energies in collodion. The fitted value of R_x/R_s is constant at 1.05 for all energies and σ_{rel} is almost uniformly found to be 0.05. The main energy-variable parameter is the threshold in $\cos\theta$ (C_{min}) which varies systematically with E. The smoothing applied to the threshold σ_C is uniformly set equal to the threshold value.

8. The modified *spherical range* model fits to the transmission data of Seliger [10] for a range of high electron energies in aluminium (159keV – 336keV). σ_{rel} and σ_C are found to be constant over the range while R_x/R_s and C_{min} vary systematically.

9. In this graph the spherical range model is compared with the transmission versus electron energy data sets (copper foil thickness (W) is constant) of Coslett and Thomas [4]. For this purpose a fixed value of σ_{rel} (0.33) is assumed and range energy ($R_s=0.007083E^{1.65}$) derived from the fits of figure 5 is used.

10. The *spherical range* for electrons in copper (from fits of figure 5) is compared with the *extrapolated range* from references [4] and [9] as a function of electron

energy.

11. The *spherical range* for electrons in gold (from fits of figure 6) is compared with the *extrapolated range* from references [4] and [9] as a function of electron energy. The range defined only by the inelastic scattering (R_0) and calculated in the continuously slowing down approximation [16] is also shown for comparison.

12. The R_x/R_s ratio for the four materials studied as a function of the electron energy (E) in the range covered by the experimental data.

13. A plot of the relative variance of the *spherical range* (σ_{rel}^2) values obtained from the fits on collodion, aluminium, copper and gold as a function of the multiple scattering parameter Z^2/A (A is the atomic number).

14. A plot of the KLL auger escape efficiency (ε_A) from a nickel surface as calculated by the spherical range model as a function of the linear absorption coefficient (μ) just above the K edge energy. The different parameters assumed are indicated in the legends: using the simple spherical model with the standard R_x (squares), the simple spherical model, R_s with σ_{rel}=0.0 (triangles) and the full spherical model, R_s with σ_{rel}=0.4 (circles). A linear fit to the lower end of a curve is shown to highlight the saturation of the signal near the K edge (μ=0.3μm^{-1}).

15. A comparison of the predictions of the simple spherical model for the x-ray fluorescent electron energy spectra from a nickel surface with the pulse height spectra observed in the gas microstrip detector in which the nickel sample is irradiated [14]. The two spectra are taken, respectively with the x-ray beam energy just below and jut on the K absorption edge.

FIGURE 1

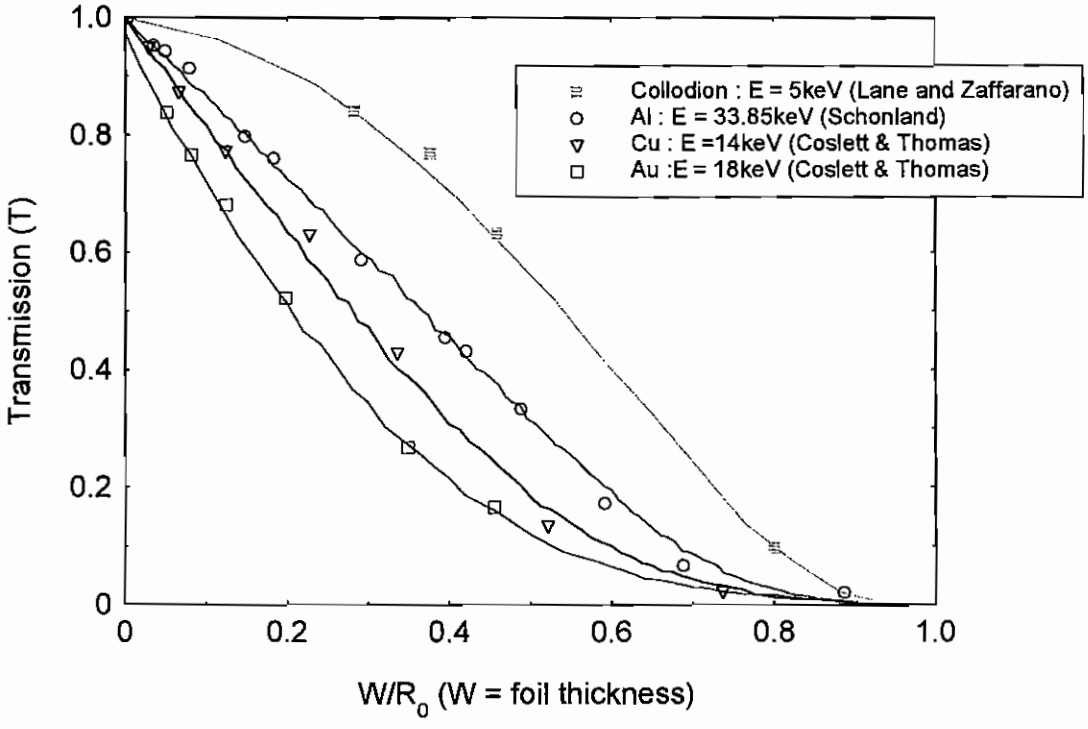

FIGURE 2

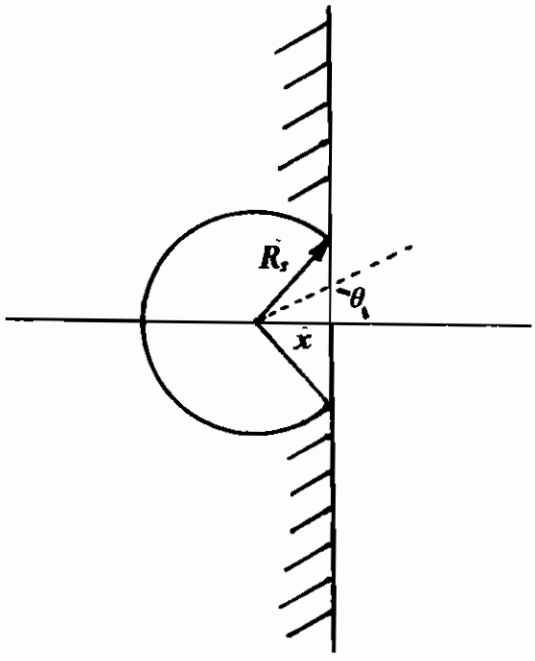

FIGURE 3

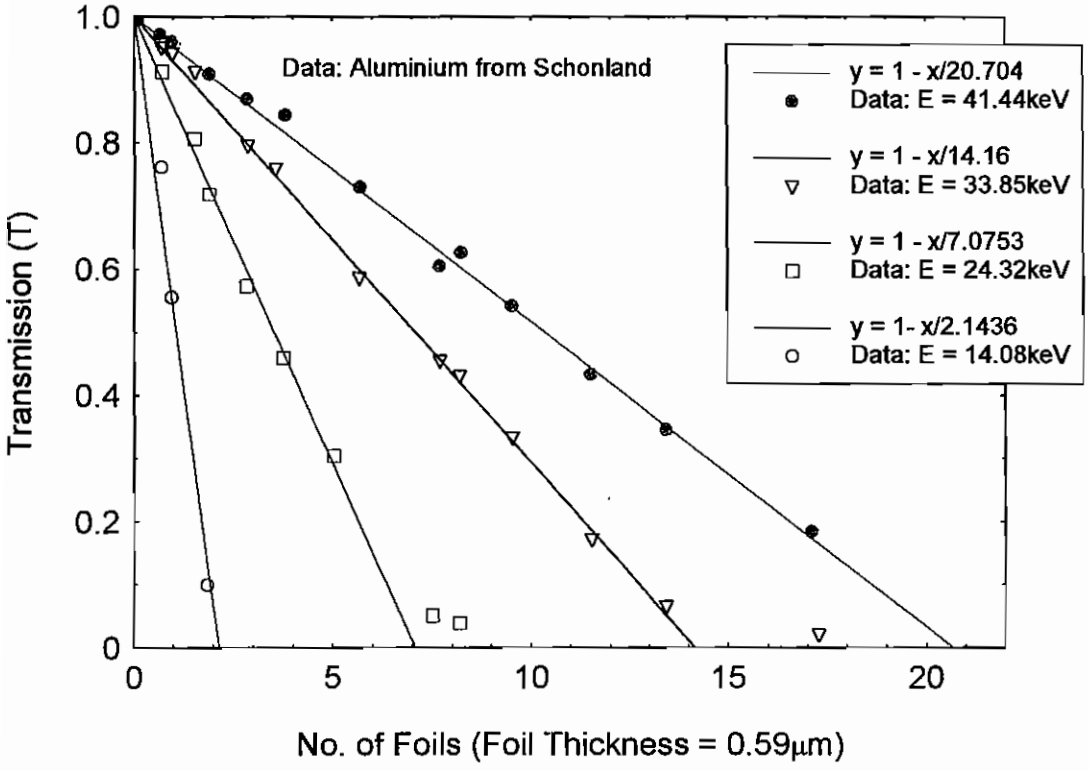

FIGURE 4

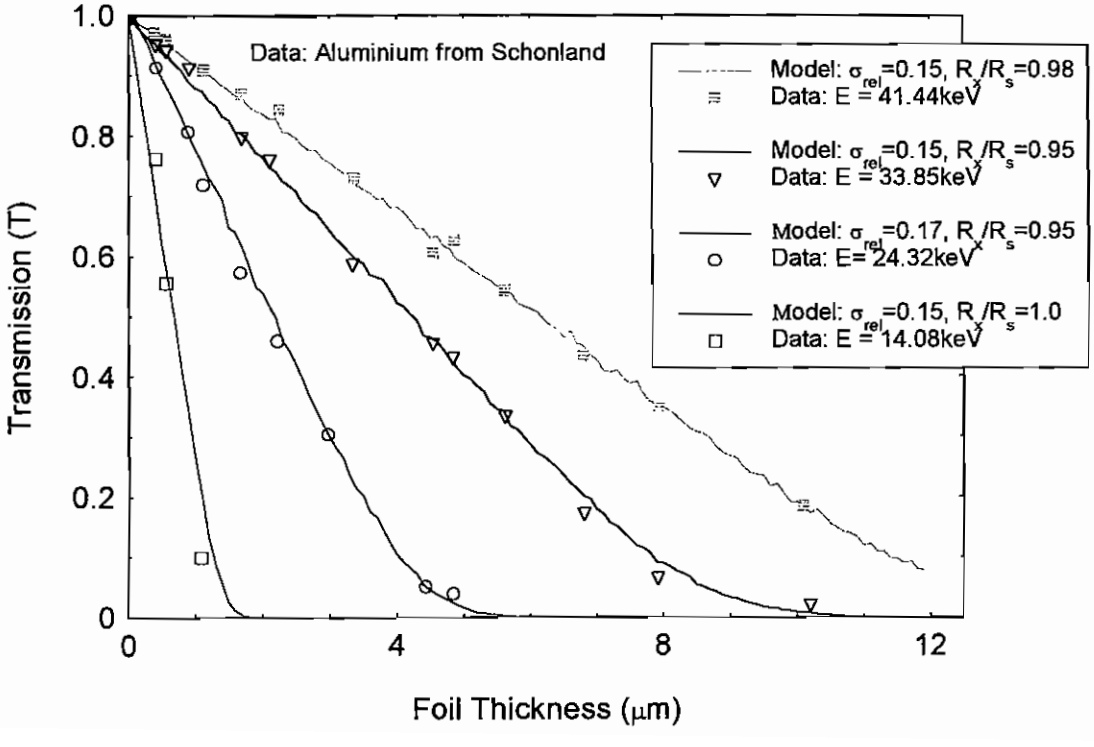

FIGURE 5

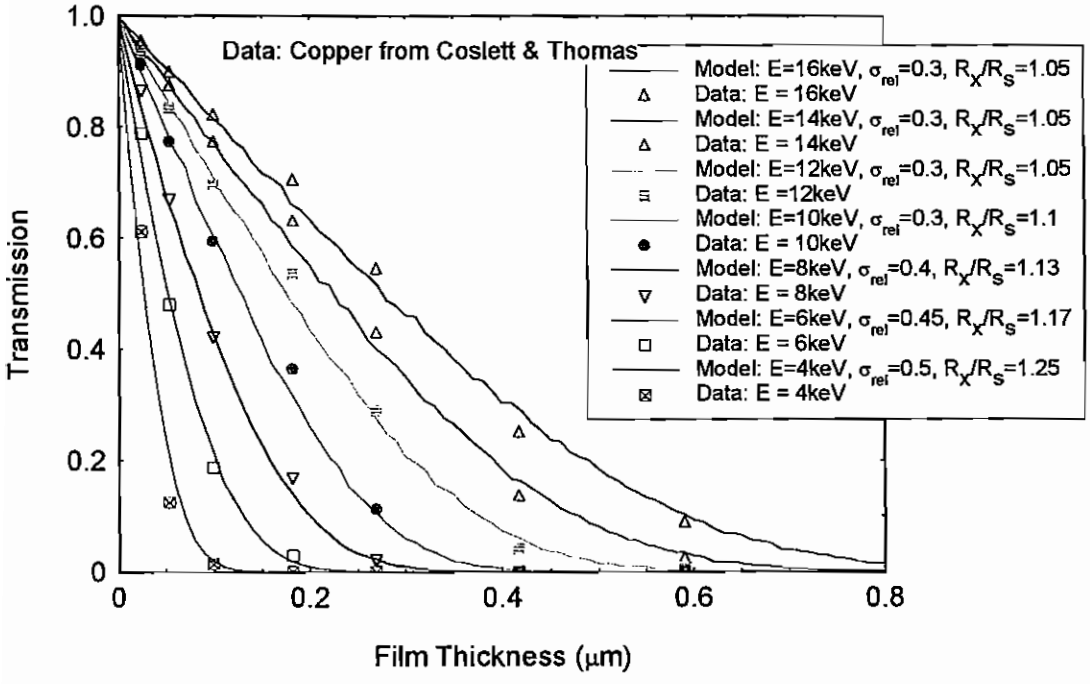

FIGURE 6

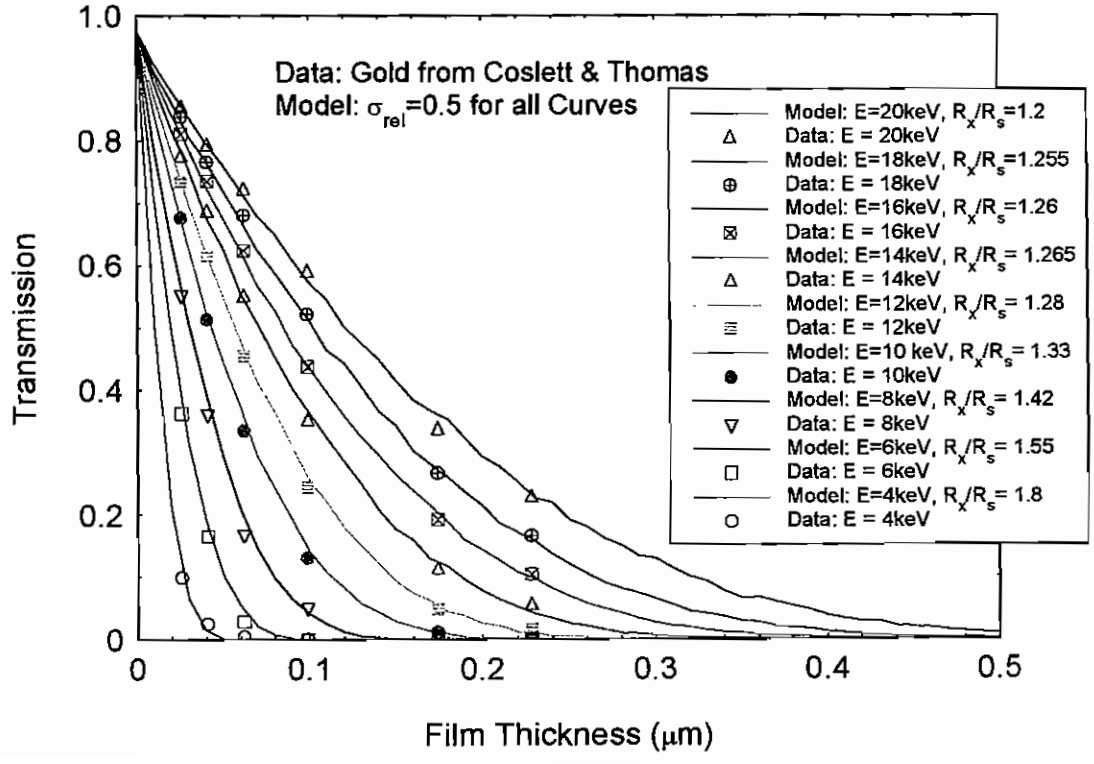

FIGURE 7

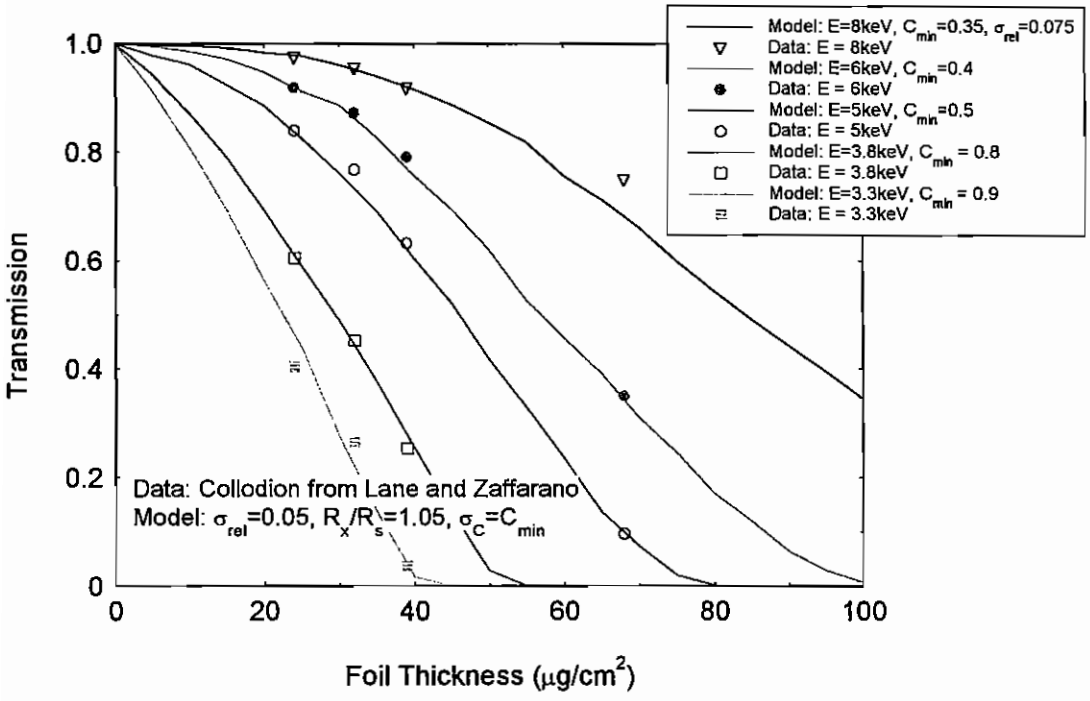

FIGURE 8

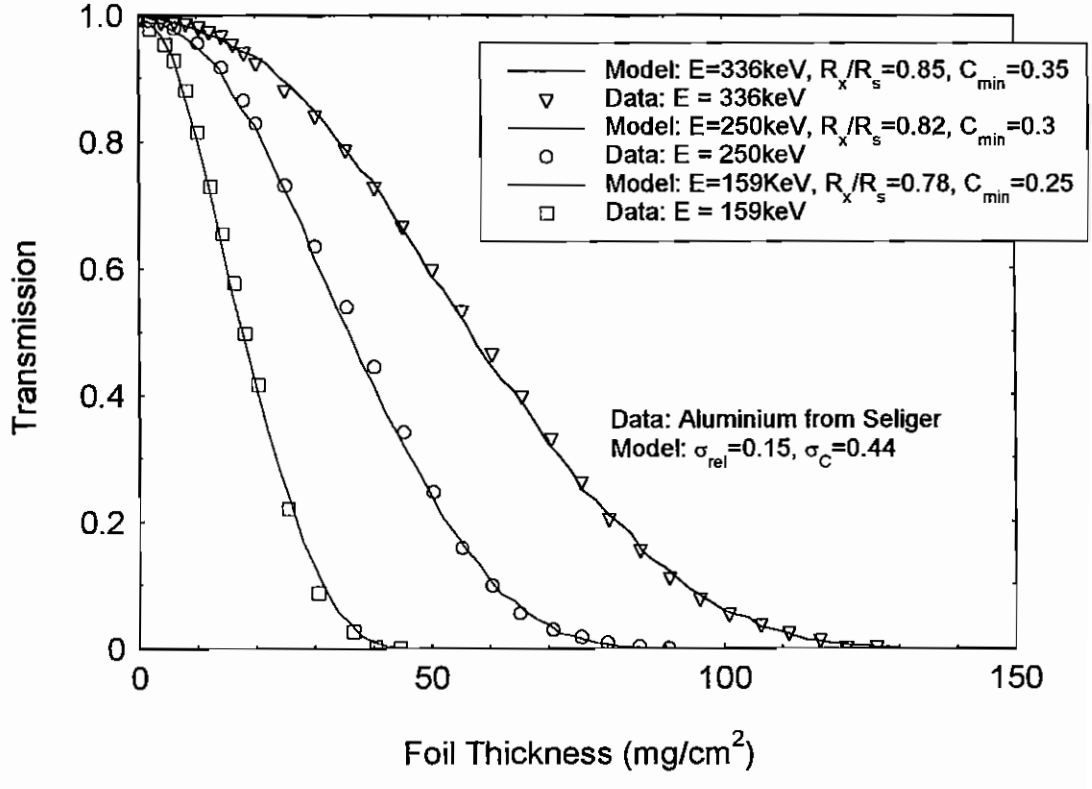

FIGURE 9

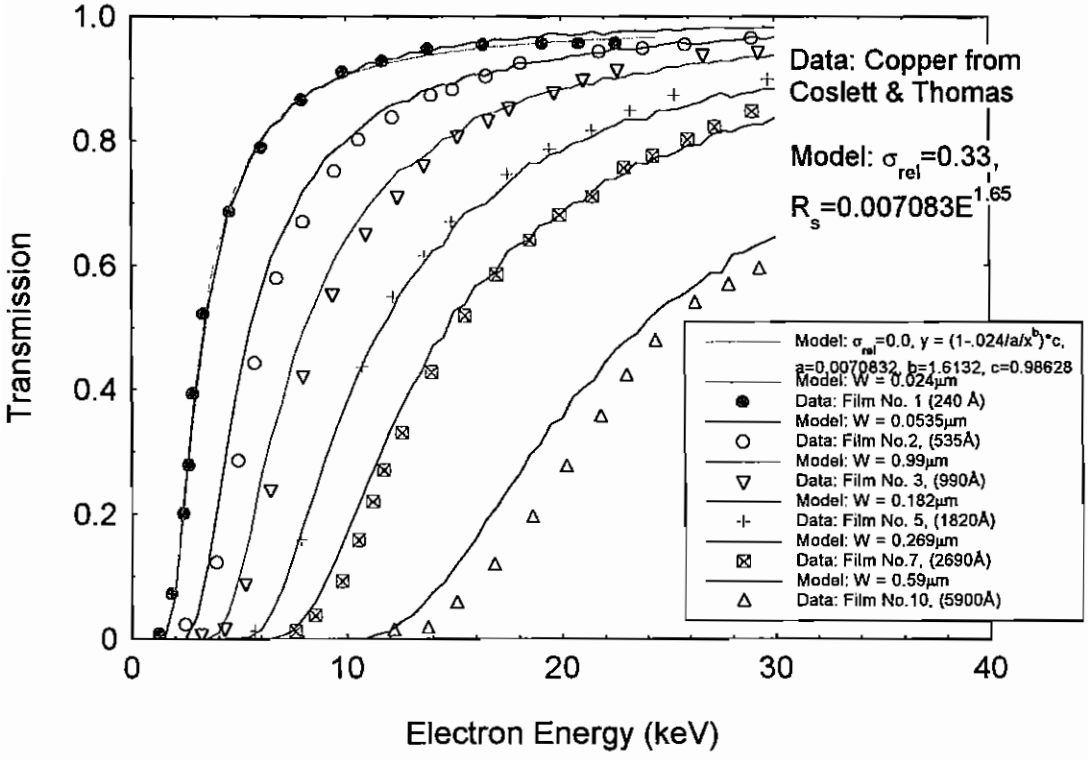

FIGURE 10

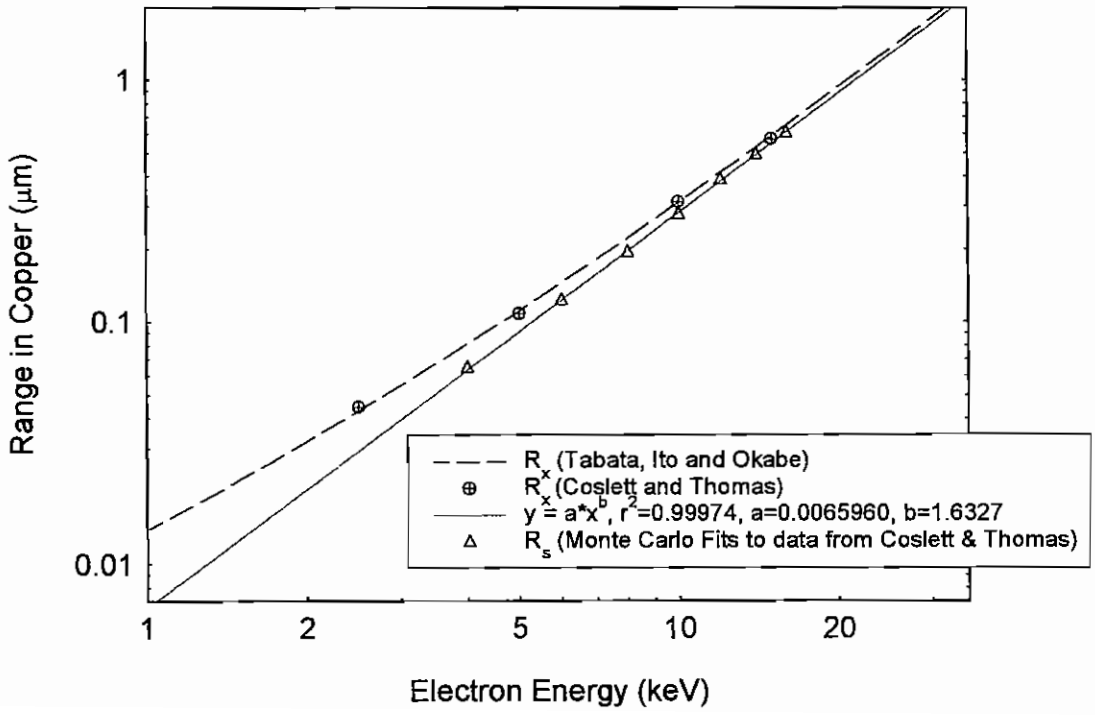

FIGURE 11

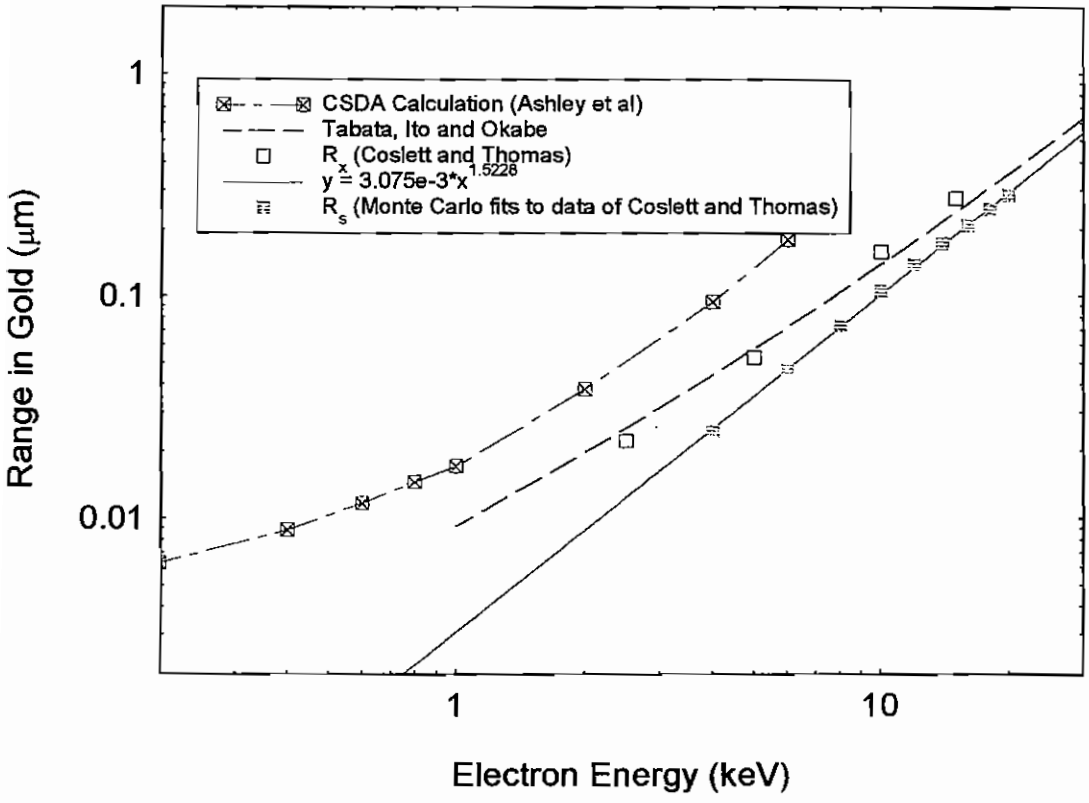

FIGURE 12

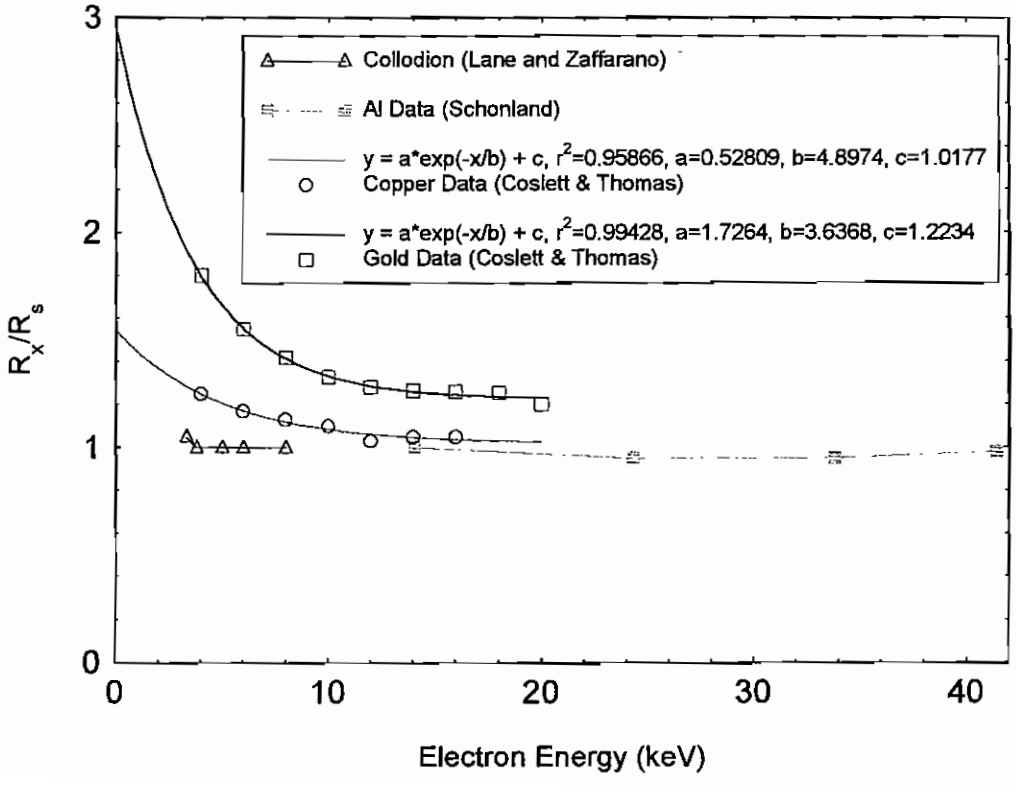

FIGURE 13

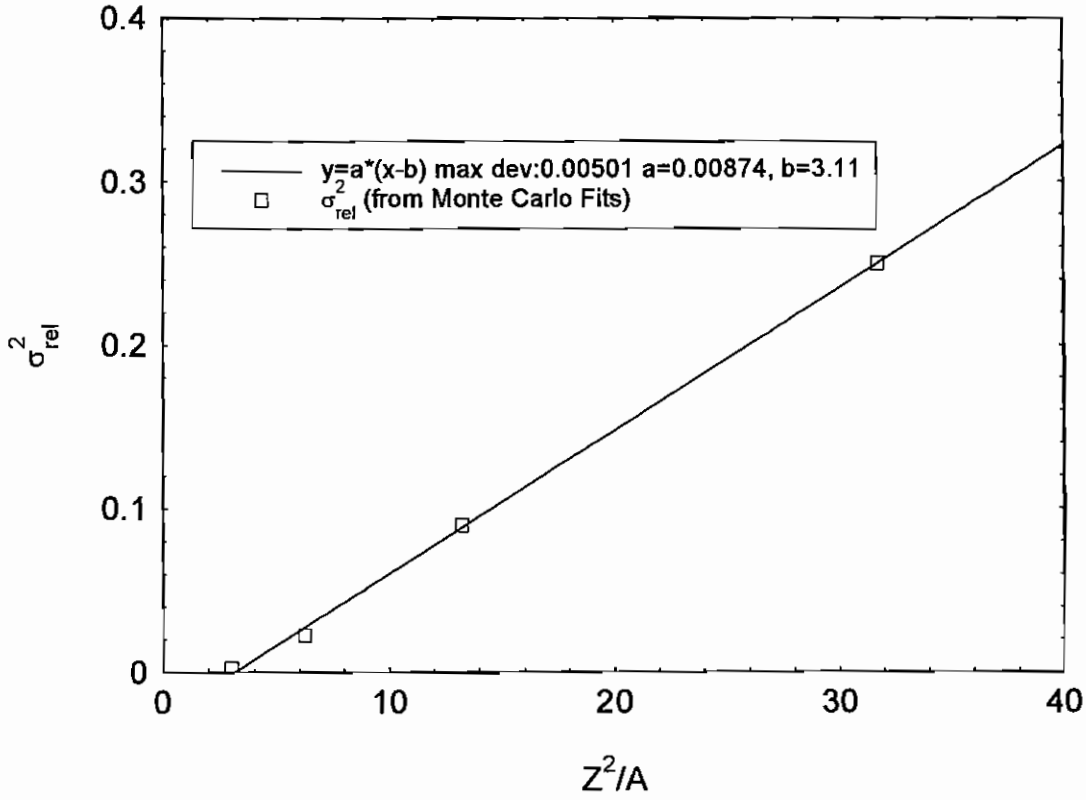

FIGURE 14

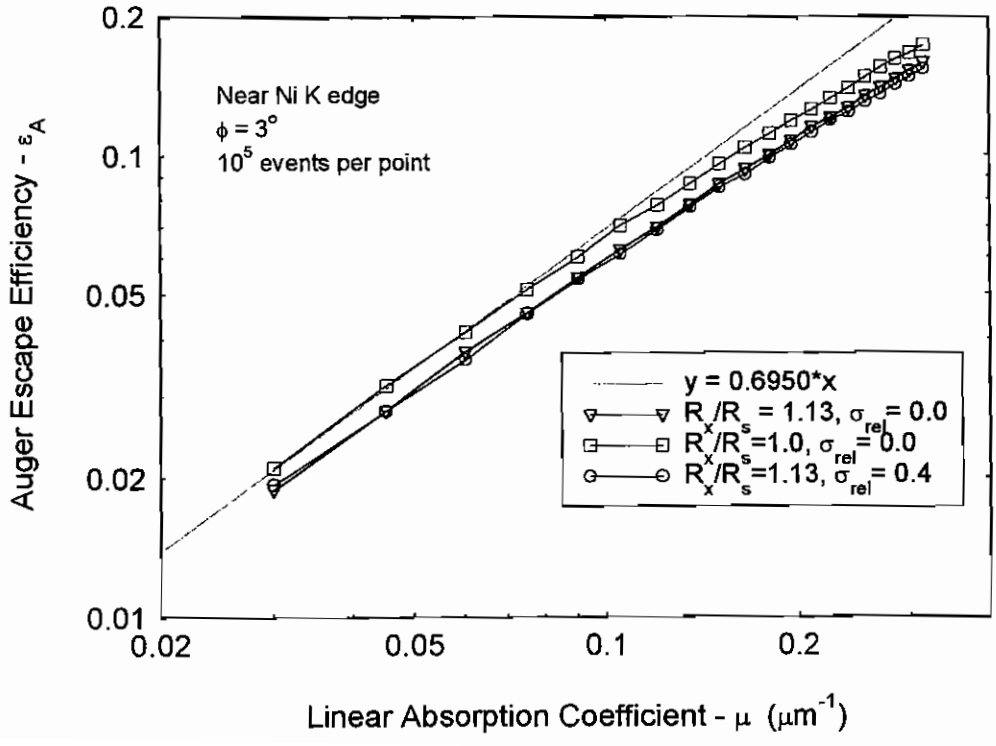

FIGURE 15

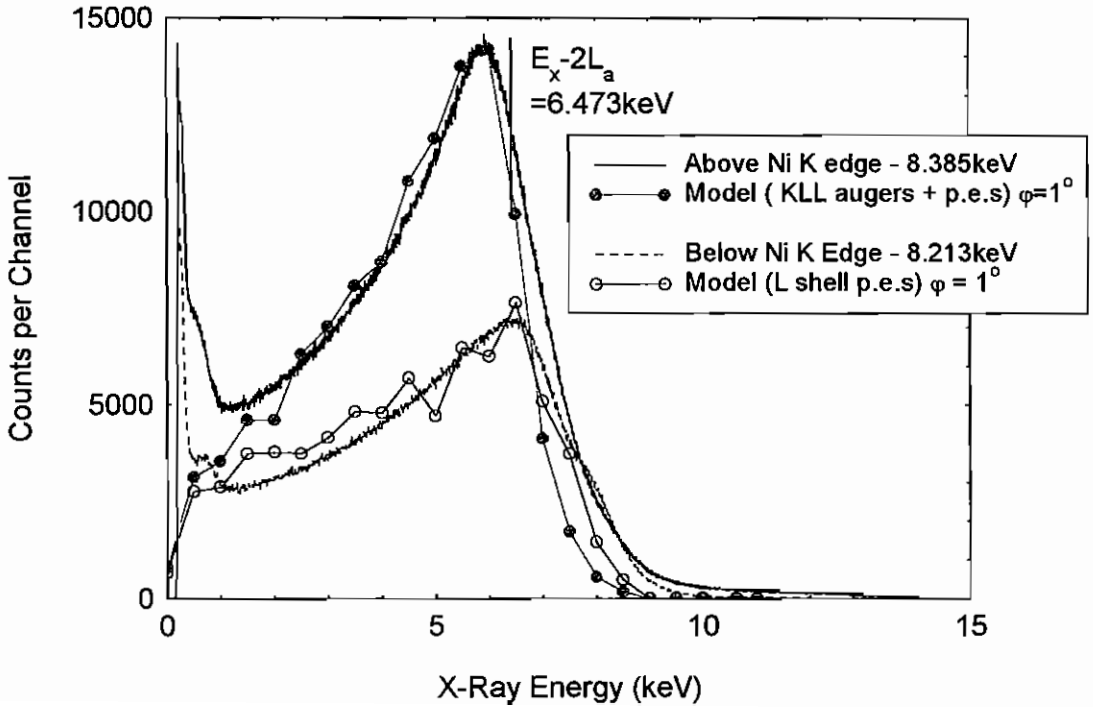
15000
10000
5000
0
0
5
10
15
Counts per Channel
X-Ray Energy (keV)
E_x-2L_a
=6.473keV
Above Ni K edge - 8.385keV
Model (KLL augers + p.e.s) φ=1°
Below Ni K Edge - 8.213keV
Model (L shell p.e.s) φ = 1°